Statistical Forecasts for the Occurrence of Precipitation Outperform Global Models over Northern Tropical Africa

Peter Vogel[1,2], Peter Knippertz[1], Tilmann Gneiting[2,3], Andreas H. Fink[1], Manuel Klar[3*], and Andreas Schlueter[1†]

[1]Institute of Meteorology and Climate Research, Karlsruhe Institute of Technology, Germany
[2]Heidelberg Institute for Theoretical Studies, Heidelberg, Germany
[3]Institute for Stochastics, Karlsruhe Institute of Technology, Germany

Key Points:

- Raw and statistically postprocessed global ensembles fail to predict West African rainfall occurrence.
- A logistic regression model using observations from preceding days outperforms all other forecasts.
- The skill is mainly related to propagating African easterly waves and mesoscale convective systems.

*currently at Department of Mathematics, Trier University, Trier, Germany
†currently at Department of Computer Science, Stanford University, Stanford, California, USA

Corresponding author: Peter Knippertz, peter.knippertz@kit.edu

Abstract

Short-term global ensemble predictions of rainfall currently have no skill over northern tropical Africa when compared to simple climatology-based forecasts, even after sophisticated statistical postprocessing. Here we demonstrate that statistical forecasts for the probability of precipitation based on a simple logistic regression model have considerable potential for improvement. The new approach we present here relies on gridded rainfall estimates from the Tropical Rainfall Measuring Mission for July–September 1998–2017 and uses rainfall amounts from the pixels that show highest positive and negative correlations on the previous two days as input. Forecasts using this model are reliable and have a higher resolution and better skill than climatology-based forecasts. The good performance is related to westward propagating African easterly waves and embedded mesoscale convective systems. The statistical model is outmatched by the postprocessed dynamical forecast in the dry outer tropics only, where extratropical influences are important.

Plain Language Summary

Forecasts of precipitation for the next few days based on state-of-the-art weather models are currently inaccurate over northern tropical Africa, even after systematic forecast errors are corrected statistically. In this paper, we show that we can use rainfall observations from the previous two days to improve predictions of precipitation occurrence. Such an approach works well over this region, as rainfall systems tend to travel from east to west organized by flow patterns several kilometers above the ground, called African easterly waves. This statistical forecast model requires training over a longer time period (here 19 years) to establish robust relationships on which future predictions can be based. The input data employed are gridded rainfall estimates based on satellite data for the African summer monsoon in July to September. The new method outperforms all other methods currently available on a day-to-day basis over the region, except for the dry outer tropics, where influences from midlatitudes, which are better captured by weather models, become more important.

1 Introduction

Large parts of tropical Africa depend on rain-fed agriculture (Wani et al., 2009). Accurate precipitation forecasts on the 1–5-day timescale could help improve many aspects of the farmers' day-to-day work such as ploughing, planting, (usually small-scale) irrigation, harvest, and livestock management. Other areas that would benefit from improved rainfall information include hydropower energy production, water resource management, disease and flood prevention as well as road safety. Arguably such information are currently much more valuable practically than decadal or climate projections (Singh et al., 2018).

A recent paper by Vogel et al. (2018) investigated the skill of nine global ensemble prediction systems participating in TIGGE (Bougeault et al., 2010) to forecast precipitation over northern tropical Africa during the extended summer monsoon season (01 May to 15 October) 2007–2014. The model forecasts were compared against a so-called extended probabilistic climatology (EPC), essentially an ensemble prediction constructed from past observations for a given calendar day along with a 2-day window around that date. It was found that raw ensemble forecasts from all nine models (and the multi-model ensemble) are uncalibrated and unreliable, and underperform in the prediction of occurrence and amount of precipitation when compared to EPC. This assessment holds for the three investigated subregions West and East Sahel and Guinea Coast, and is robust against accumulation periods from 1 to 5 days and grid spacings from $0.25°\times0.25°$ to $2°\times5°$. Consistent results were found for the satellite-based Tropical Rainfall Measur-

ing Mission (TRMM) 3B42 gridded product and raingauge data from the Karlsruhe African Surface Station Database (KASS-D).

To improve the model forecasts, the two state-of-the-art statistical postprocessing methods Ensemble Model Output Statistics (EMOS) (Gneiting et al., 2005; Scheuerer, 2014) and Bayesian Model Averaging (BMA) (Raftery et al., 2005; Sloughter et al., 2007) were applied by Vogel et al. (2018). Both consistently improve the forecasts' calibration and reliability but the overall predictive performance is hardly better than that of EPC. Only the multi-model ensemble shows slightly positive skill for all eight investigated years. Vogel et al. (2018) speculate that this sobering result is related to the fact that the convective parametrizations used in global models struggle to realistically represent mesoscale convective systems (MCSs), which largely dominate the rainfall generation in the region (Mathon et al., 2002; Fink et al., 2006; Maranan et al., 2018). This deficit has been shown to also deteriorate larger-scale circulations on timescales of five days and more in numerical weather prediction models (Marsham et al., 2013; Pante & Knippertz, 2019). An extension of the analysis by Vogel et al. (2018) to the entire tropical belt from 30°S and 30°N (Vogel et al., manuscript to be submitted to *Weather and Forecasting*) shows that tropical Africa stands out to have the lowest predictive skill – even after postprocessing – of all tropical continents. This result holds for rainfall occurrence, amount, and extremes at accumulation periods of 1 to 5 days. The fact that this region is exceptional in its degree of convective organization (Nesbitt et al., 2006; Roca et al., 2014) supports its potential role in forecast degradation (Vogel et al., 2018).

While the results summarized above are disappointing and require further investigation, they also call for the development of alternative approaches. Various studies have shown that rainfall over tropical Africa is by no means as erratic as the low model skill suggests, but is in fact modulated on the synoptic to planetary scale by tropical wave phenomena, most prominently African easterly waves (AEWs) (Schlueter, Fink, Knippertz, & Vogel, 2019). The dominant influence of AEWs on precipitation over West Africa has been known for several decades (Reed et al., 1977; Mekonnen et al., 2006; Lavaysse et al., 2006). According to Fink and Reiner (2003), more than 60% of MCSs in West Africa are associated with AEWs. The combination of quasi-linear waves that influence the occurrence and propagation of long-lived MCSs via modulations of lower tropospheric shear, midlevel relative humidity, and convective available potential energy (CAPE) (Schlueter, Fink, & Knippertz, 2019) points to potential forecast improvements through statistical models based on spatio-temporal correlation patterns in observations. Such models may outperform dynamical models, as these struggle to represent the coupling between convection and tropical waves (Elless & Torn, 2018; Dias et al., 2018) and at the same time display higher sharpness and resolution than EPC due to knowledge of the current atmospheric situation. To test this hypothesis, here we present results for a probabilistic forecast model for precipitation occurrence over northern tropical Africa based on a simple logistic regression approach. Statistical forecast methods were more common at times when computational power was more limited, but the concept has largely been abandoned as numerical weather prediction has become increasingly skillful in the extratropics (Wilks, 2019, Section 7.9.1). A famous example of a statistical forecast is the so-called "Yesterday" method that is based on observations from preceding days and was used in tropical Africa in the mid 20th century (Schove, 1946). However, we are unaware of any recent study of statistical approaches to (synoptic) rainfall forecasting in Africa.

The following Section 2 gives an overview of the employed data and methods. In Section 3 the spatio-temporal correlation of precipitation is analyzed, forming the basis for a statistical forecast method and its evaluation in Section 4. Finally, Section 5 presents the main conclusions and an outlook.

2 Data and methods

Our study is based on the TRMM 3B42-V7 gridded product (Huffman et al., 2007) that is used for the creation of an EPC, for forecast validation, and the development of statistical forecasts. TRMM merges active measurements from the precipitation radar with passive, radar-calibrated information from infrared as well as microwave measurements. The precipitation estimates are calibrated against nearby gauge observations on a monthly basis. The TRMM data are available on a $0.25° \times 0.25°$ grid with 3-hourly temporal resolution but were accumulated here to daily sums and to $1° \times 1°$ gridboxes. The spatial aggregation, however, had little impact on the obtained spatio-temporal correlations (not shown). The investigations are focused on the core summer monsoon season (July–September) for the 20 years from 1998–2017. The study region is northern tropical Africa from 25°W–50°E and 3–18°N (corresponding to the area shown in Fig. 4). All investigations are made for the probability of precipitation (PoP), for which we set a threshold of 0.2 mm per day. The satellite-based rainfall data are used to construct an EPC forecast with a ±2-day window as in Vogel et al. (2018).

For comparison, we include corresponding forecasts from the Integrated Forecasting System of the European Centre for Medium-Range Weather Forecasts (ECMWF) for the years since 2011, subsequent to a major increase in the resolution of the model grid. See `https://www.ecmwf.int/en/publications/ifs-documentation` for a comprehensive documentation. Data were downloaded on the standard reduced Gaussian grid and then regridded with the Climate Data Operator (CDO) software to $1° \times 1°$ to match the TRMM data. As Vogel et al. (2018) showed substantial improvement when applying statistical postprocessing to the raw ensemble forecasts, we include here also ECMWF forecasts postprocessed using the EMOS method consistent with their results.

The statistical forecast will follow a simple strategy. For each TRMM gridbox, we analyze the relationship between 1-day accumulated precipitation at the location considered, and rainfall amounts at just any gridbox one and two days before, using Spearman's rank correlation. This allow us to identify the locations with the strongest statistical relationships (both in a positive and negative sense), which we then use to construct the statistical model. Specifically, let o_1^+, o_2^+, o_1^-, and o_2^- denote the observations at lags of one and two days at the strongest positively and negatively correlated gridboxes, respectively. We employ a logistic regression model of the form

$$\text{logit}(p) \mid o_1^+, o_2^+, o_1^-, o_2^-, d \;=\; a_1^+ f(o_1^+) + a_2^+ f(o_2^+) + a_1^- f(o_1^-) + a_2^- f(o_2^-) + s(d), \qquad (1)$$

for the forecast probability p, where $\text{logit}(p) = \log(p/(1-p))$. The function $f(x) = \log(x+0.001)$ transforms a nonnegative precipitation amount to the real line, and the term

$$s(d) \;=\; b_0 + b_1 \sin(2\pi d/365) + b_2 \cos(2\pi d/365) \qquad (2)$$

depends on the day of the year d in a periodic fashion. To train such a model one needs to distinguish between verification and training data. When issuing predictions for a July–September period in a given year, observations from that year are used for verification, while observations from all other years from within 1998–2017 are used for training. So altogether, the following steps are conducted for each gridbox: We (a) find Spearman's rank correlations from the training data to identify the locations with the highest positive and negative correlation coefficients at lags of one and two days, (b) estimate the parameters a_1^+, a_2^+, a_1^-, a_2^-, b_0, b_1, and b_2 of the statistical model in Eqs. 1 and 2 with the iteratively reweighted least squares technique, and (c) compute PoP forecasts for each day of the verification period based on the values of $o_1^+, o_2^+, o_1^-, o_2^-$, and d at hand.

For EMOS, we follow common practice, use a rolling training period of the most recent 500 days, comprising data from both the gridbox at hand and the eight neighboring gridboxes, provided they share the respective land/water characteristic, and apply the estimation methods described by Scheuerer (2014) and Vogel et al. (2018). So ul-

timately, four different types of PoP forecasts are generated and compared in this paper: a climatological prediction (termed EPC), raw model ensemble output (ENS), a post-processed model prediction (EMOS), and a purely statistical forecast (Logistic).

3 Spatio-temporal correlation of precipitation

To illustrate the statistical forecast method, an example application is discussed here for Niamey. In Figure 1 the panels at left show Spearman's rank correlation results for July–September 1998–2017. At a lag of a single day, precipitation at Niamey is most strongly correlated (above the 99th percentile of the correlation coefficients in the study region) with an east–west extended, spatially coherent region along the eastern part of the border between Niger and Nigeria. The pixel with the highest value overall, which is used in the logistic regression model, is located at 13.5°N and 10.5°E and thus almost exactly 8 degrees (ca. 900 km) to the east of Niamey. This propagation speed is slightly faster than that of a typical AEW of 9.1 ms^{-1} (ca. 800 km per day) but considerably slower than that of a typical MCS of 15 ms^{-1} (ca. 1300 km per day) (Fink & Reiner, 2003). The corresponding analysis for a lag of two days shows a further shift of the area of highest correlation upstream to a maximum located at 14.5°N and 19.5°E, corresponding to a distance of about 1000 km and thus in good agreement with the behavior on the previous day. The correlation values are lower but the extremal region remains spatially coherent. Overall, this supports our assumption that information on recent rainfall events propagates with MCSs and AEWs. The fact that the relationship is robust over two days points to a key role of AEW propagation for convection, as MCSs typically have shorter lifetimes of around 12h (Fink & Reiner, 2003).

In contrast, the strongest negative correlations are found to the south of Niamey for both lags. For the first day, the region is fairly coherent and stretches from southwestern Ghana to southeastern Burkina Faso, culminating in northern Togo. For the second day, there is much less spatial coherence and the most extreme value occurs over northwestern Nigeria and thus much closer to Niamey than for the positive correlations. The interpretation of the negative correlation results is less clear. It is conceivable that they also reflect AEW influence on precipitation indicating suppression in the downstream ridge. Knippertz et al. (2017) documented regional north–south fluctuations in rainfall associated with propagating disturbances during the DACCIWA campaign in June–July 2016. Another possibility is a north–south shift in the monsoonal rainfall belt as discussed on subseasonal (Janicot et al., 2011) and interannual (Nicholson, 2008) time scales.

The center and right-hand side panels in Figure 1 illustrate the modulation of the PoP at Niamey conditional on the accumulated precipitation amounts at the highest positively correlated locations at lags of one and two days (denoted o_1^+ and o_2^+ in Eq. 1). We categorize these precipitation amounts into no, light, and strong rainfall. The top center panel displays the PoP at Niamey conditional on the categorical precipitation at lag one day. From an average climatological value of 0.50 (marked by black lines), the PoP reduces to 0.42 for no precipitation at a lag of one day at the location marked with a cross in the top left panel and increases to 0.71 if strong precipitation occurred there. For a lag of two days (bottom right panel), the range of deviations from climatology decreases only slightly with values of 0.44 and 0.68, respectively. Considering both observations jointly (bottom center panel) reveals even stronger modulations of the PoP. If at both lags no precipitation was observed at the respective locations, the PoP at Niamey falls to 0.37, while it is 0.81, thus more than double, for strong precipitation on both previous days. This clearly illustrates the potential in our approach.

4 Statistical forecasts for the occurrence of precipitation

Based on the correlation results discussed in the previous section, Figure 2 displays a July–September 2016 time series of logistic regression-based forecasts for Niamey (Lo-

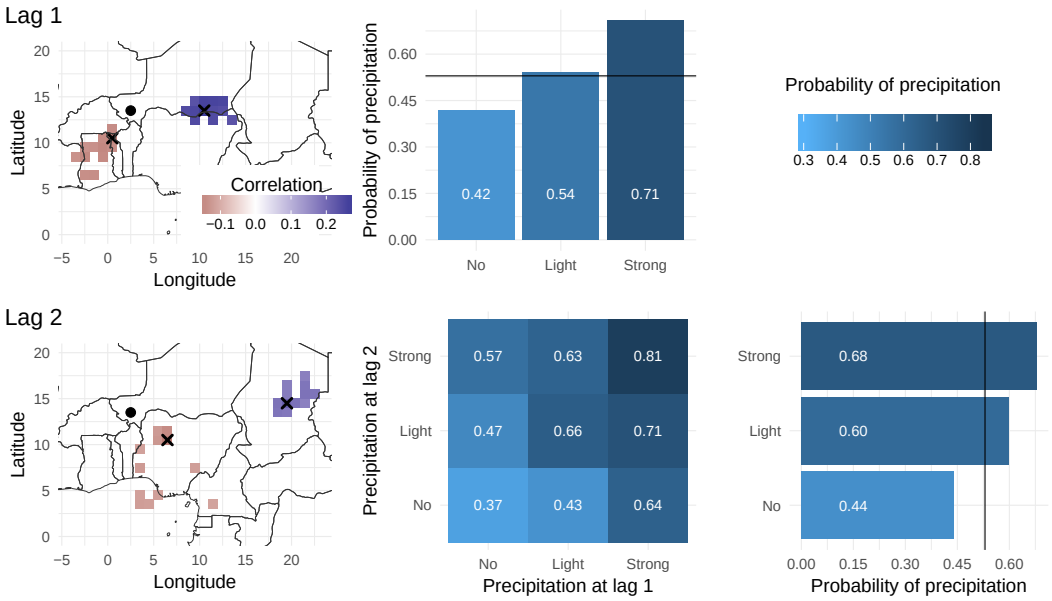

Figure 1. Spatio-temporal correlation of precipitation for the gridbox of Niamey (black dot). Displayed are the strongest 1% of positive (blue) and negative (red) correlations between 1-day accumulated precipitation at Niamey and surrounding gridboxes at lags of one (top left) and two (bottom left) days, based on Spearman's rank correlation and the period July–September 1998–2017, with the locations of the highest and lowest values overall indicated by crosses. The center bottom panel shows the PoP at Niamey conditional on both 1- and 2-day lagged categorized precipitation values, while the neighboring panels show the corresponding marginally conditioned probabilities. The black lines mark the climatological PoP of 0.50. The categories of light and strong rainfall are separated by the climatological median of the non-zero precipitation amounts.

gistic, blue line) in comparison with the direct ECMWF model output (ENS, black dots), postprocessed ECMWF predictions (EMOS, orange line), and the climatology-based forecast (EPC, red line). The actual observed rainfall occurrence is marked with grey shading.

The EPC forecast reflects the average annual cycle with PoP increasing from 0.50 at the beginning of July to a maximum of about 0.67 in mid-August and a fall-off to 0.30 at the end of September, which is associated with the advance and retreat of the West African monsoon. Observations in 2016 roughly correspond with this seasonal evolution showing frequent rainfall with longer wet periods in mid-July and mid-August, and a tendency towards drier conditions in September. The ENS forecast reveals an obvious tendency to forecast rainfall occurrence with certainty (i.e., with probability 1.00), while lower PoPs are generally rare. EMOS postprocessing changes this dramatically to a PoP prediction that follows the seasonal cycle reflected in EPC, while taking into account the tendencies for drier or wetter conditions evident in ENS. Finally Logistic shares many of the characteristics evident in EMOS but varies more strongly from about 0.20 to 0.80. This indicates an overall better resolution of Logistic.

The procedure demonstrated in Figures 1 and 2 was repeated for all other years of our comparison period July–September 2011–2017. Figure 3 shows the resulting reliability diagrams, where the observed relative frequency is plotted versus the forecast probability in 10% bins (blue lines). The inset histograms indicate the number of cases in the bins. The ENS forecast confirms the impression from Figure 2 that the raw en-

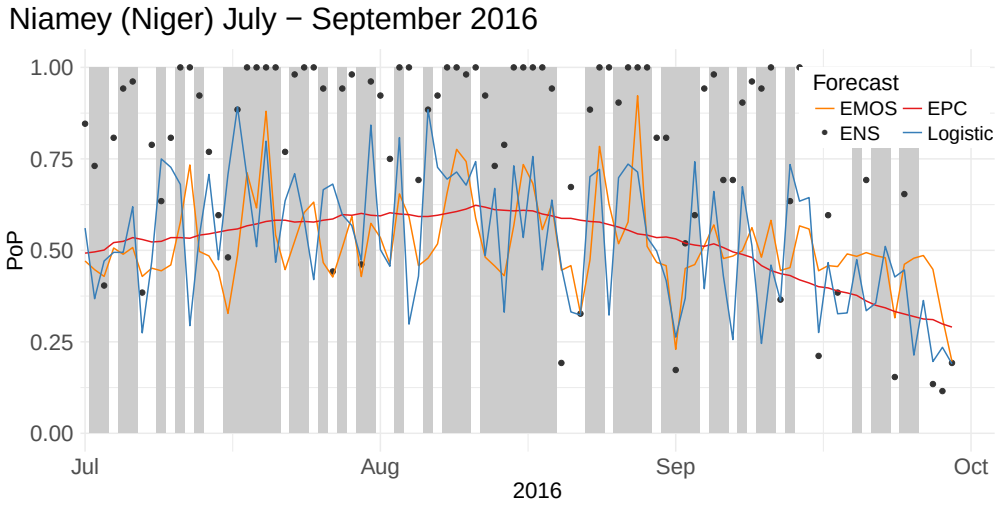

Figure 2. ENS (black dots), EMOS (orange line), EPC (red line), and Logistic (blue line) forecasts for the occurrence of precipitation at the gridpoint of Niamey (marked with a dot in the left panels of Figure 1) during July–September 2016, and the actual occurrence of precipitation indicated by grey shading. For a description of the different forecast types, see Section 2.

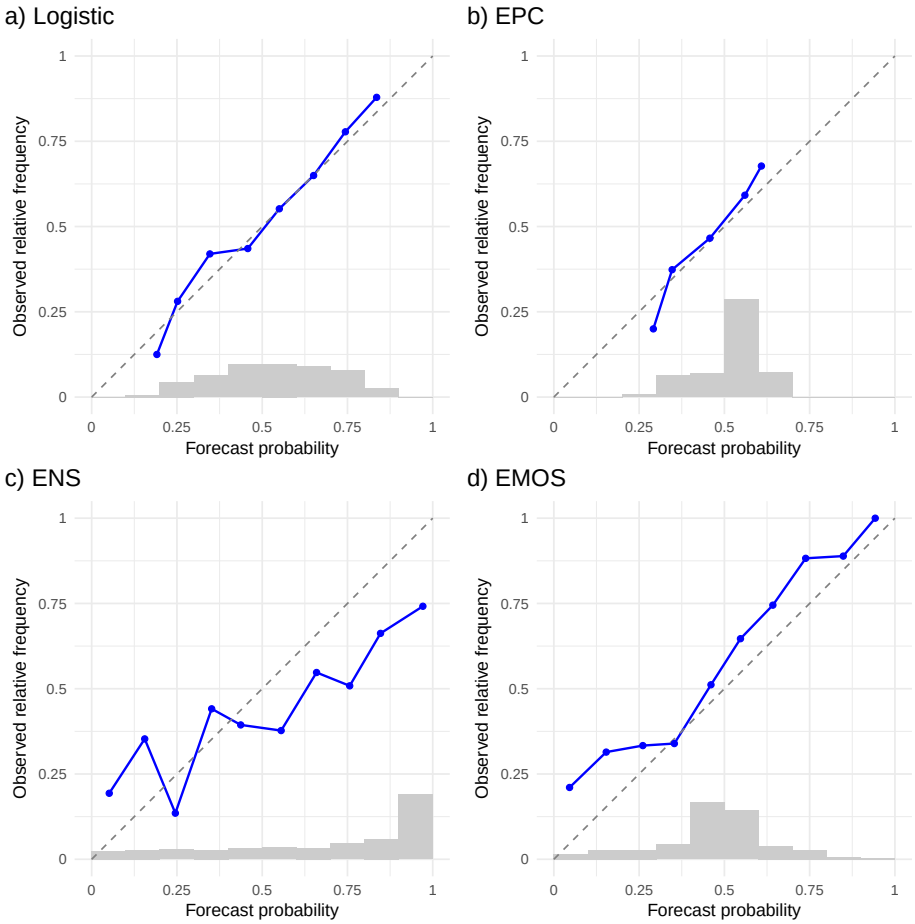

Figure 3. Reliability diagrams for a) Logistic, b) EPC, c) ENS, and d) EMOS forecasts of PoP at the gridpoint of Niamey for July–September 2011–2017.

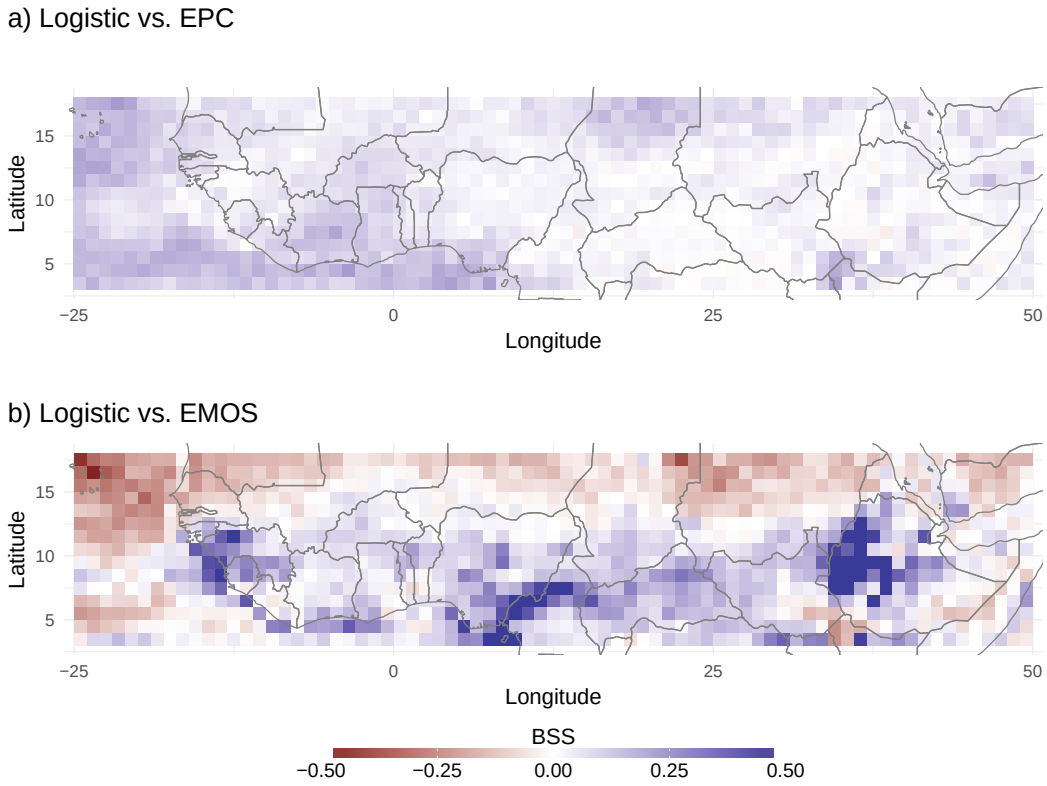

Figure 4. Spatial display of the Brier skill score (BSS) for Logistic relative to a) EPC and b) EMOS forecasts for July–September 2011–2017.

semble frequently predicts rain with certainty, which however only verifies in about 75% of the respective cases (Figure 3, panel c). The other forecast probability bins are relatively uniformly populated, hinting at good resolution. However, the reliability of ENS is unsatisfactory with overall too wet conditions for dry forecasts and vice versa. EPC displays much better reliability but low resolution with forecast probabilities only varying between 0.25 and 0.65. The EMOS forecast clearly combines elements of EPC and ENS (panels b–d). Despite the noisiness inherited from ENS, reliability is much improved, while resolution is reduced through the influence of climatological information. Finally, the Logistic forecast (panel a) clearly shows the most superior forecasts with reliability similar to EPC but much higher resolution.

In order to gauge the predictive performance of the Logistic forecast on the regional scale, we extend the approach exemplified above for Niamey to all gridboxes in the study region for July–September 2011–2017. Panel a in Figure 4 displays the spatial distribution of the Brier skill score (BSS) of the Logistic forecast relative to EPC. It shows that skill increases – or stays the same – over all of northern tropical Africa and the adjacent tropical Atlantic Ocean. The spatial average of the BSS amounts to 0.061, with values for individual gridboxes ranging from -0.039 to 0.239. There is no obvious geographical pattern to the improvement, apart perhaps from a slight tendency for higher values in the west where AEWs are usually more intense and couple more strongly to organized convection (Fink & Reiner, 2003). Land-ocean contrasts may also play a role.

Panel b shows the BSS relative to EMOS. Here a much clearer geographical pattern emerges. Improvements are pronounced over terrestrial areas to the south of about 13°N, while the northern Sahel and southern Sahara as well as oceanic areas mostly show

a degradation of the forecast. Our example gridbox at Niamey is located close to the border between these areas, where forecast improvement by Logistic over EMOS is neutral. The spatial average is still positive at 0.038 but reduced compared to the BSS relative to EPC. This pattern suggests that Logistic outperforms EMOS where AEWs have a strong influence on daily rainfall (Schlueter, Fink, Knippertz, & Vogel, 2019), a connection that is known to be ill represented in dynamical models (Marsham et al., 2013; Pante & Knippertz, 2019). An additional factor appears to be problems with orographic precipitation in the ECMWF model, as Logistic is particularly superior over all major mountain areas of the southern zone, i.e., the Ethiopian Highlands, the Cameroon Line Mountains, and the Guinea Highlands in the far west. In these areas the BSS reaches values of more than 0.50, even though one would expect orographic effects to be systematic enough to be corrected for by postprocessing. This result therefore requires a more in-depth analysis, which is beyond the scope of this paper.

The relatively poor performance in the dry region to the north suggests that the occasional rainfalls in this area are not primarily caused by meridionally propagating waves that have been shown to lose their influence to the north of 15°N (Schlueter, Fink, Knippertz, & Vogel, 2019). Past case studies suggest that here precipitation is often associated with anomalous influences from the extratropics (Cuesta et al., 2010; Roehrig et al., 2011; Vizy & Cook, 2014) and it is plausible that these are better represented by a dynamical model due to their rather episodic nature. At locations near the extratropical boundary of our study region, propagating signals from the north cannot be represented by the statistical model. It is interesting to note that the good performance of EMOS is most pronounced over the ocean around the Cape Verde Islands, a region that is known to be affected by upper-level troughs from the midlatitudes, even occasionally in the summer half year (Fröhlich & Knippertz, 2008).

These results demonstrate that no single method alone can resolve the problem of poor dynamical model performance over northern tropical Africa and that future work should try attempting to blend dynamical and statistical information in an optimal way.

5 Conclusions

Motivated by the poor performance of dynamical forecast models to predict rainfall over northern tropical Africa, we have demonstrated that it is possible to construct skillful statistical forecasts for precipitation occurrence on the basis of information about recent rainfall events alone. The method we have developed uses gridded precipitation data from TRMM for the period July–September 1998–2017. For a given location and day, we first identify pixels with the strongest positive and negative correlations on the previous days from a training dataset. Rainfall amounts at these locations and times have then be employed to train a logistic regression model for rainfall occurrence at the target location and time. This model is ultimately used to make forecasts for a verification period. The predictions obtained this way are then compared to a probabilistic forecast based on climatology (EPC) as well as raw and postprocessed ensemble predictions from the ECMWF. The main conclusions from this analysis are:

- The statistical forecasts are reliable and have higher resolution than climatology-based forecasts, as they take the current weather situation into account.
- They outperform EPC forecasts over most of northern tropical Africa and the adjacent Atlantic Ocean with an area-mean BSS of 0.06.
- Exemplary correlation patterns and the geographical distribution of forecast skill of the statistical model suggest that westward propagation of AEWs and MCSs, possibly together with synoptic-scale latitudinal shifts in the monsoon system, are underlying reasons for the good performance.
- Over areas where precipitation is more sporadic and more strongly influenced by the usually more predictable extratropical circulation, such as the northern Sa-

hel/southern Sahara and the adjacent Atlantic Ocean, the statistical model is outperformed by postprocessed ensemble predictions based on the ECMWF model.

To our knowledge, the results presented are the first-ever demonstration of successful short-term statistical rainfall forecasts over the region and we advocate that such approaches be considered as an attractive alternative to the widely distributed direct model output. It should be noted, however, that such a model (in particular such a simple one) can only work if there is a strong and consistent physical mode that dominates rainfall variability. In other regions where rainfall is more chaotic and/or several wave modes superimpose, our approach will likely not be as powerful as over West Africa. Nevertheless, this initial success provides strong motivation to expand the concept to (a) precipitation amounts, (b) other tropical regions, (c) longer leadtimes, (d) other rainfall datasets (particularly as TRMM is not active anymore), (e) more sophisticated statistical techniques (in particular convolutional neural networks that allow exploiting the full spatio-temporal correlation pattern, possibly even including interactions of different wave types), and (f) additional input data (e.g., moisture or wind variables). This can ultimately help to meet the large challenge to create a hybrid forecast system that combines the strengths of dynamical models, postprocessing, and statistical forecasting in an optimal way.

Acknowledgments

The research leading to these results has been accomplished within project C2 "Prediction of wet and dry periods of the West African Monsoon" of the Transregional Collaborative Research Center SFB/TRR 165 "Waves to Weather" funded by the German Science Foundation (DFG). TG is grateful for support by the Klaus Tschira Foundation. TRMM data are available at `https://pmm.nasa.gov/data-access/downloads/trmm`. ECMWF forecast data are available at `https://www.ecmwf.int/en/forecasts/datasets`.

References

Bougeault, P., Toth, Z., Bishop, C., Brown, B., Burridge, D., Chen, D. H., ... Worley, S. (2010). The THORPEX interactive grand global ensemble. *Bull. Amer. Meteorol. Soc.*, *91*(8), 1059-1072. doi: 10.1175/2010BAMS2853.1

Cuesta, J., Lavaysse, C., Flamant, C., Mimouni, M., & Knippertz, P. (2010). Northward bursts of the West African monsoon leading to rainfall over the Hoggar Massif, Algeria. *Quart. J. Roy. Meteorol. Soc.*, *136*(s1), 174–189. doi: 10.1002/qj.439

Dias, J., Gehne, M., Kiladis, G. N., Sakaeda, N., Bechtold, P., & Haiden, T. (2018). Equatorial waves and the skill of NCEP and ECMWF numerical weather prediction systems. *Mon. Wea. Rev.*, *146*(6), 1763–1784. doi: 10.1175/MWR-D-17-0362.1

Elless, T. J., & Torn, R. D. (2018). African Easterly Wave forecast verification and its relation to convective errors within the ECMWF ensemble prediction system. *Wea. Forecasting*, *33*(2), 461–477. doi: 10.1175/WAF-D-17-0130.1

Fink, A., & Reiner, A. (2003). Spatiotemporal variability of the relation between African easterly waves and West African squall lines in 1998 and 1999. *J. Geophys. Res.*, *108*, 4332. doi: 10.1029/2002JD002816

Fink, A., Vincent, D., & Ermert, V. (2006). Rainfall types in the West African Sudanian zone during the summer monsoon 2002. *Mon. Wea. Rev.*, *134*, 2143–2164. doi: 10.1175/MWR3182.1

Fröhlich, L., & Knippertz, P. (2008). Identification and global climatology of upper-level troughs at low latitudes. *Meteorol. Zeitschrift*, *17*(5), 565–573. doi: 10.1127/0941-2948/2008/0320

Gneiting, T., Raftery, A. E., Westveld, A. H., & Goldman, T. (2005). Calibrated probabilistic forecasting using ensemble model output statistics

and minimum CRPS estimation. *Mon. Wea. Rev.*, *133*, 1098–1118. doi: 10.1175/MWR2904.1

Huffman, G. J., Bolvin, D. T., Nelkin, E. J., Wolff, D. B., Adler, R. F., Gu, G., ... Stocker, E. F. (2007). The TRMM multisatellite precipitation analysis (TMPA): Quasi-global, multiyear, combined-sensor precipitation estimates at fine scales. *J. Hydrometeorol.*, *8*(1), 38–55. doi: 10.1175/JHM560.1

Janicot, S., Caniaux, G., Chauvin, F., de Coëtlogon, G., Fontaine, B., Hall, N., ... Taylor, C. M. (2011). Intraseasonal variability of the West African monsoon. *Atmos. Sci. Lett.*, *12*(1), 58–66. doi: 10.1002/asl.280

Knippertz, P., Fink, A., Deroubaix, A., Morris, E., Tocquer, F., Evans, M., ... Schlueter, A. (2017). A meteorological and chemical overview of the DACCIWA field campaign in West Africa in June–July 2016. *Atmos. Chem. Phys.*, *17*, 10893–10918. doi: 10.5194/acp-17-10893-2017

Lavaysse, C., Diedhiou, A., Laurent, H., & Lebel, T. (2006). African easterly waves and convective activity in wet and dry sequences of the West African monsoon. *Climate Dyn.*, *27*, 319–332. doi: 10.1007/s00382-006-0137-5

Maranan, M., Fink, A. H., & Knippertz, P. (2018). Rainfall types over southern West Africa: Objective identification, climatology and synoptic environment. *Quart. J. Roy. Meteorol. Soc.*, *144*, 1628–1648. doi: 10.1002/qj.3345

Marsham, J. H., Dixon, N. S., Garcia-Carreras, L., Lister, G. M. S., Parker, D. J., Knippertz, P., & Birch, C. E. (2013). The role of moist convection in the West African monsoon system – Insights from continental-scale convection-permitting simulations. *Geophys. Res. Lett.*, *40*, 1843–1849. doi: 10.1002/grl.50347

Mathon, V., Laurent, H., & Lebel, T. (2002). Mesoscale convective system rainfall in the Sahel. *J. Appl. Meteorol.*, *41*, 1081–1092. doi: 10.1175/1520-0450(2002)041⟨1081:MCSRIT⟩2.0.CO;2

Mekonnen, A., Thorncroft, C. D., & Aiyyer, A. R. (2006). Analysis of convection and its association with African easterly waves. *J. Climate*, *19*, 5405—5421. doi: 10.1175/JCLI3920.1

Nesbitt, S. W., Cifelli, R., & Rutledge, S. A. (2006). Storm morphology and rainfall characteristics of TRMM precipitation features. *Mon. Wea. Rev.*, *134*, 2702–2721. doi: 10.1175/MWR3200.1

Nicholson, S. E. (2008). The intensity, location and structure of the tropical rainbelt over west Africa as factors in interannual variability. *Int. J. Climatol.*, *28*(13), 1775–1785. doi: 10.1002/joc.1507

Pante, G., & Knippertz, P. (2019). Resolving Sahelian thunderstorms improves midlatitude weather forecasts. *Nature Comm.*, *10*(1), 3487. doi: 10.1038/s41467-019-11081-4

Raftery, A. E., Gneiting, T., Balabdaoui, F., & Polakowski, M. (2005). Using Bayesian model averaging to calibrate forecast ensembles. *Mon. Wea. Rev.*, *133*, 1155–1174. doi: 10.1175/MWR2906.1

Reed, R. J., Norquist, D. C., & Recker, E. E. (1977). The structure and properties of African wave disturbances as observed during phase III of GATE. *Mon. Wea. Rev.*, *105*, 317–333. doi: 10.1175/1520-0493(1977)105,0317:TSAPOA.2.0.CO;2

Roca, R., Aublanc, J., Chambon, P., Fiolleau, T., & Viltard, N. (2014). Robust observational quantification of the contribution of mesoscale convective systems to rainfall in the tropics. *J. Climate*, *27*(13), 4952–4958. doi: 10.1175/JCLI-D-13-00628.1

Roehrig, R., Chauvin, F., & Lafore, J.-P. (2011). 10–25 day intraseasonal variability of convection over the Sahel: a role of the Saharan heat low and midlatitudes. *J. Climate*, *24*, 5863–5878. doi: 10.1175/2011JCLI3960.1

Scheuerer, M. (2014). Probabilistic quantitative precipitation forecasting using ensemble model output statistics. *Quart. J. Roy. Meteorol. Soc.*, *140*, 1086–1096.

doi: 10.1002/qj.2183

Schlueter, A., Fink, A. H., & Knippertz, P. (2019). A systematic comparison of tropical waves over northern Africa. Part II: Dynamics and thermodynamics. *J. Climate*, *32*, 2605–2625. doi: 10.1175/JCLI-D-18-0651.1

Schlueter, A., Fink, A. H., Knippertz, P., & Vogel, P. (2019). A systematic comparison of tropical waves over northern Africa. Part I: Influence on rainfall. *J. Climate*, *32*, 1501–1523. doi: 10.1175/JCLI-D-18-0173.1

Schove, D. J. (1946). Note on equatorial forecasting technique. *Quart. J. Roy. Meteorol. Soc.*, *72*, 110–112.

Singh, C., Daron, J., Bazaz, A., Ziervogel, G., Spear, D., Krishnaswamy, J., ... Kituyi, E. (2018). The utility of weather and climate information for adaptation decision-making: current uses and future prospects in Africa and India. *Climate Develop.*, *10*(5), 389–405. doi: 10.1080/17565529.2017.1318744

Sloughter, J. M., Raftery, A. E., Gneiting, T., & Fraley, C. (2007). Probabilistic quantitative precipitation forecasting using Bayesian model averaging. *Mon. Wea. Rev.*, *135*, 3209–3220. doi: 10.1175/MWR3441.1

Vizy, E. K., & Cook, K. H. (2014). Impact of cold air surges on rainfall variability in the Sahel and wet African tropics: a multi-scale analysis. *Clim. Dyn.*, *43*, 1057–1081. doi: 10.1007/s00382-013-1953-z

Vogel, P., Knippertz, P., Fink, A. H., Schlueter, A., & Gneiting, T. (2018). Skill of global raw and postprocessed ensemble, predictions of rainfall over northern tropical Africa. *Wea. Forecasting*, *33*, 369–388. doi: 10.1175/WAF-D-17-0127.1

Wani, S., Sreedevi, T., Rockström, J., & Ramakrishna, Y. (2009). Rainfed agriculture – Past trends and future prospects. In S. Wani, J. Rockström, & T. Oweis (Eds.), *Rainfed agriculture: Unlocking the potential* (Vol. 7, pp. 1–35). Wallingford, UK.

Wilks, D. S. (2019). *Statistical methods in the atmospheric sciences* (4th ed.). Amsterdam: Elsevier.

Figure 1.

Lag 1

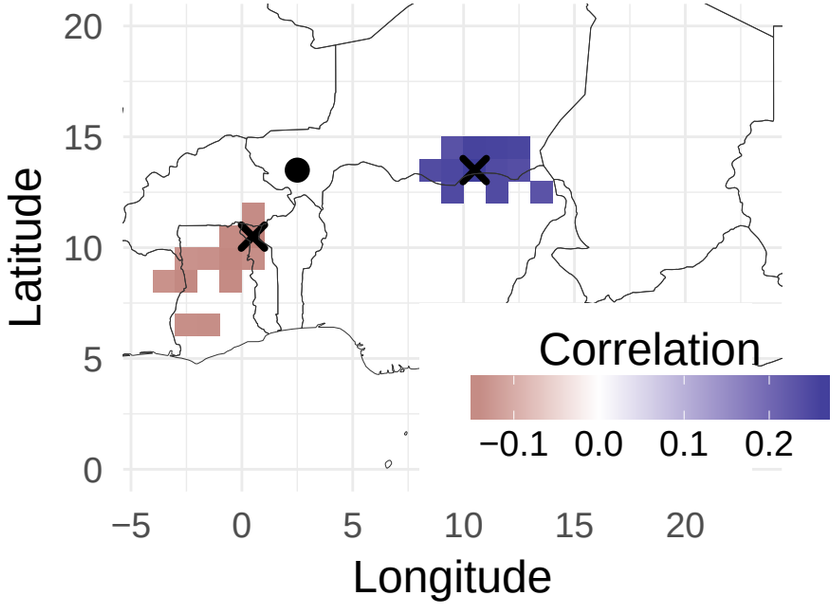
Latitude
Longitude
Correlation
−0.1 0.0 0.1 0.2

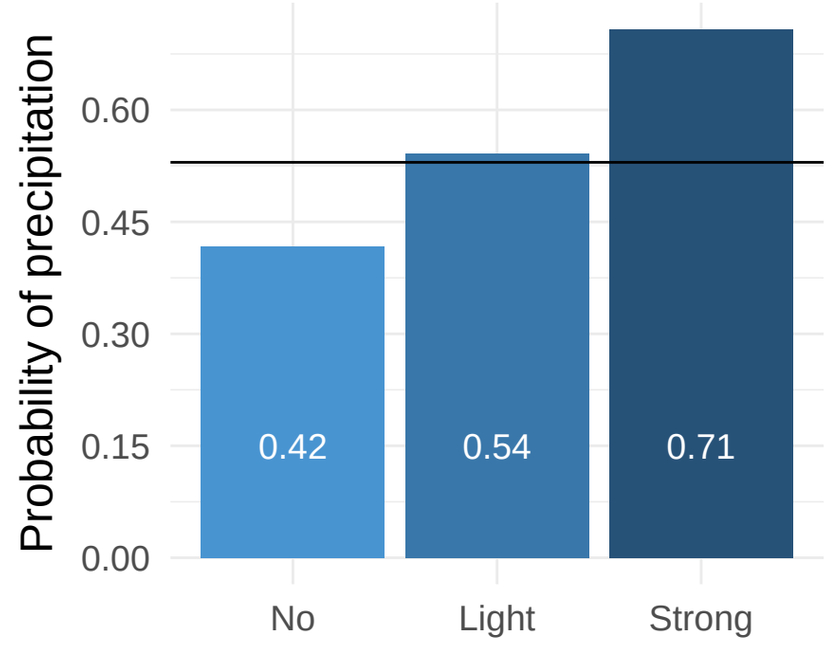
Probability of precipitation
0.42
0.54
0.71
No
Light
Strong

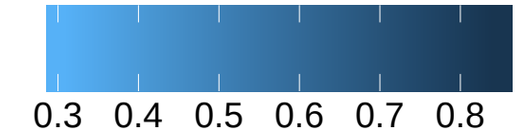
Probability of precipitation
0.3 0.4 0.5 0.6 0.7 0.8

Lag 2

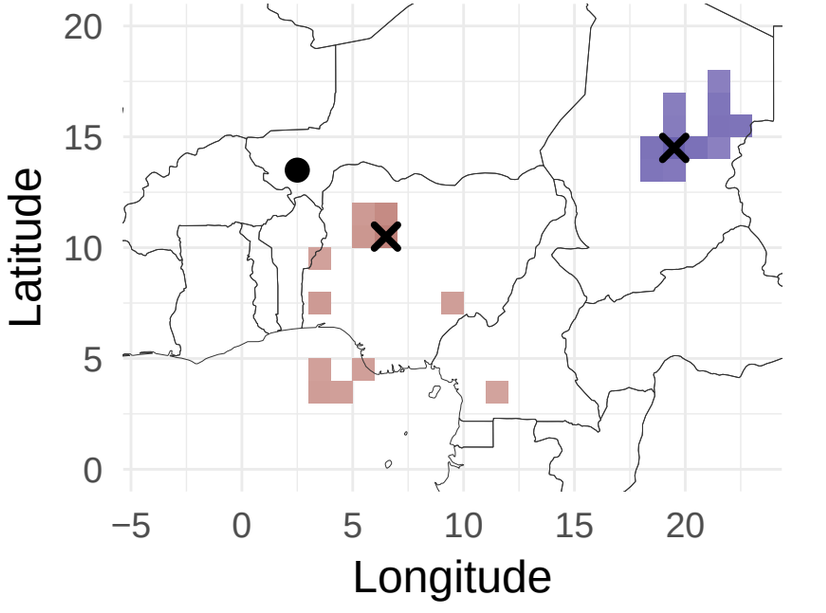
Latitude
Longitude

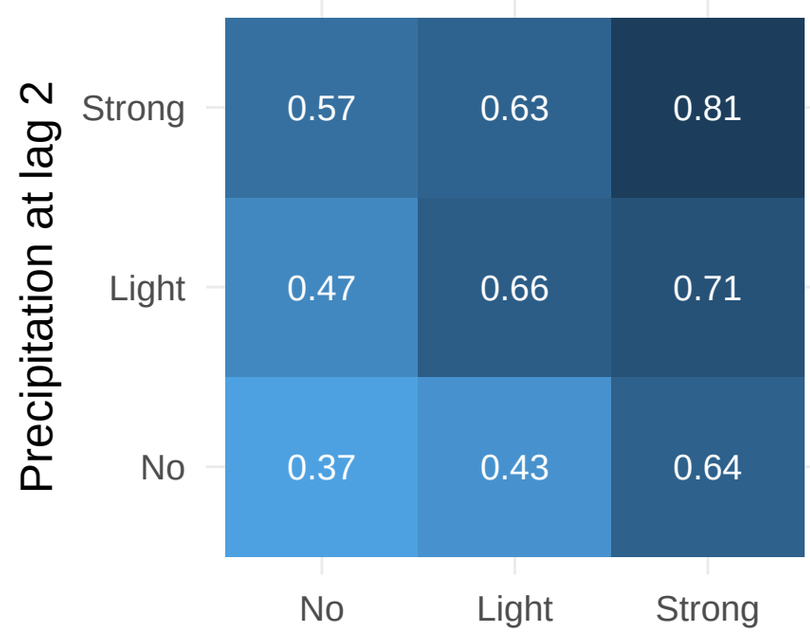
Precipitation at lag 2
Strong
Light
No
0.57 0.63 0.81
0.47 0.66 0.71
0.37 0.43 0.64
No
Light
Strong
Precipitation at lag 1

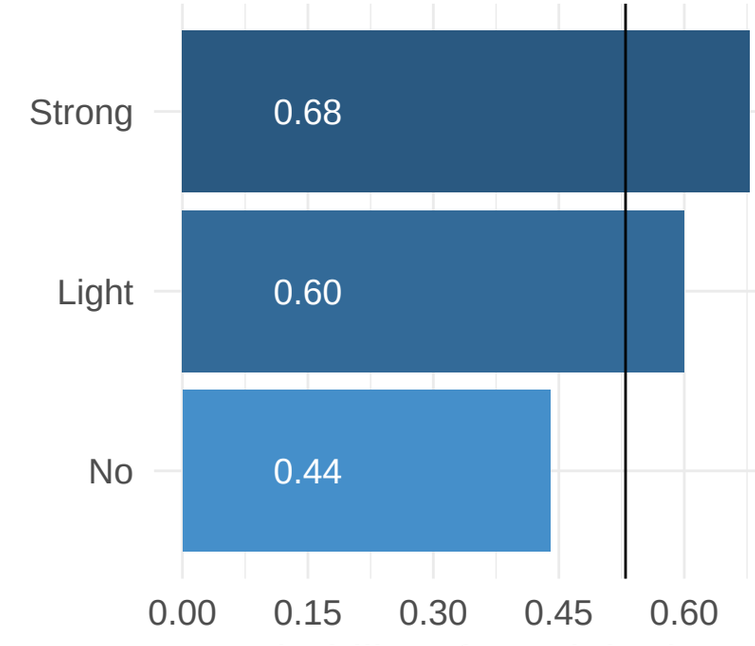
Strong
Light
No
0.68
0.60
0.44
0.00 0.15 0.30 0.45 0.60
Probability of precipitation

Figure 2.

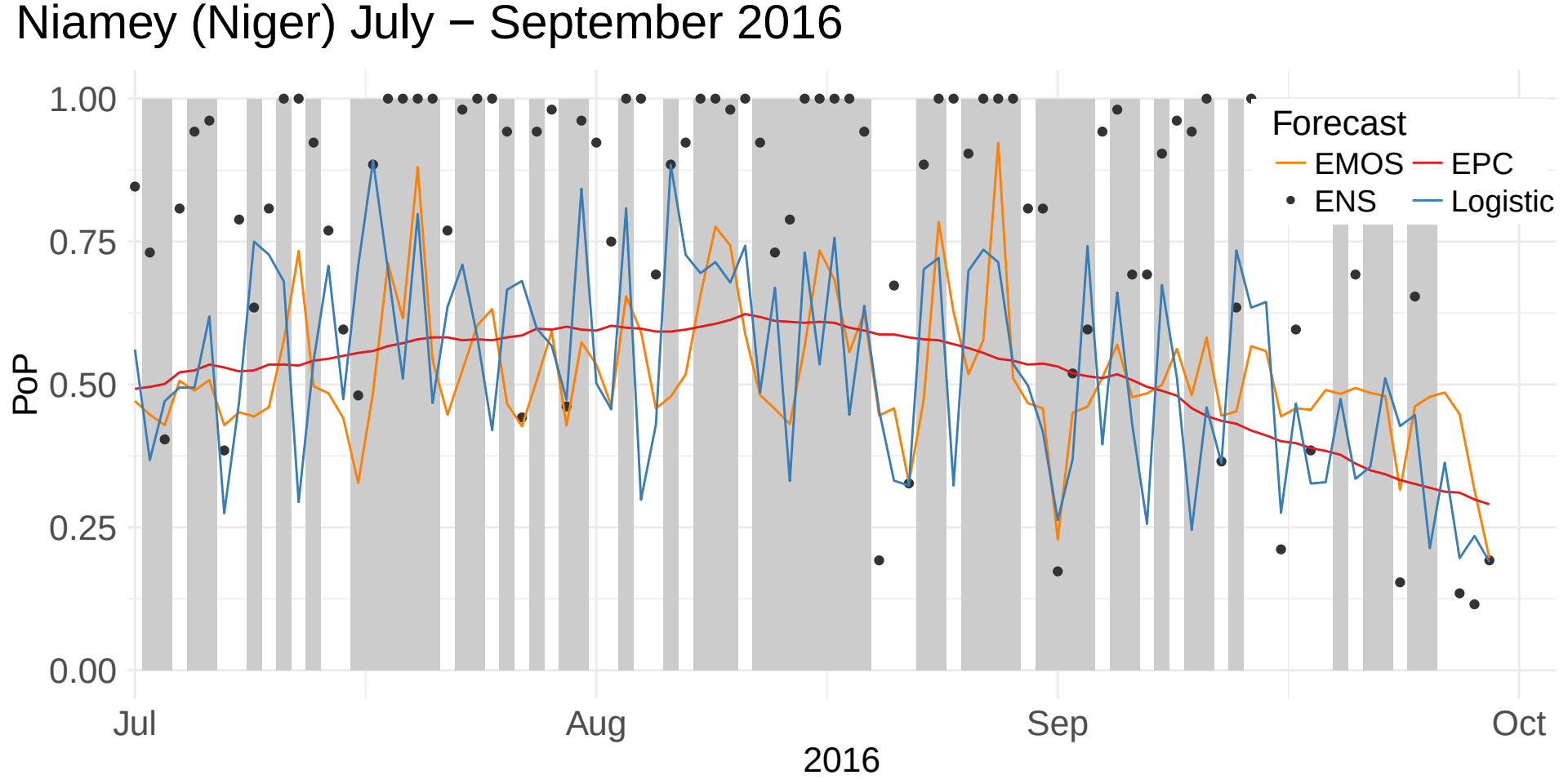
Niamey (Niger) July − September 2016
1.00
0.75
0.50
0.25
0.00
PoP
Jul
Aug
Sep
Oct
2016
Forecast
EMOS
EPC
ENS
Logistic

Figure 3.

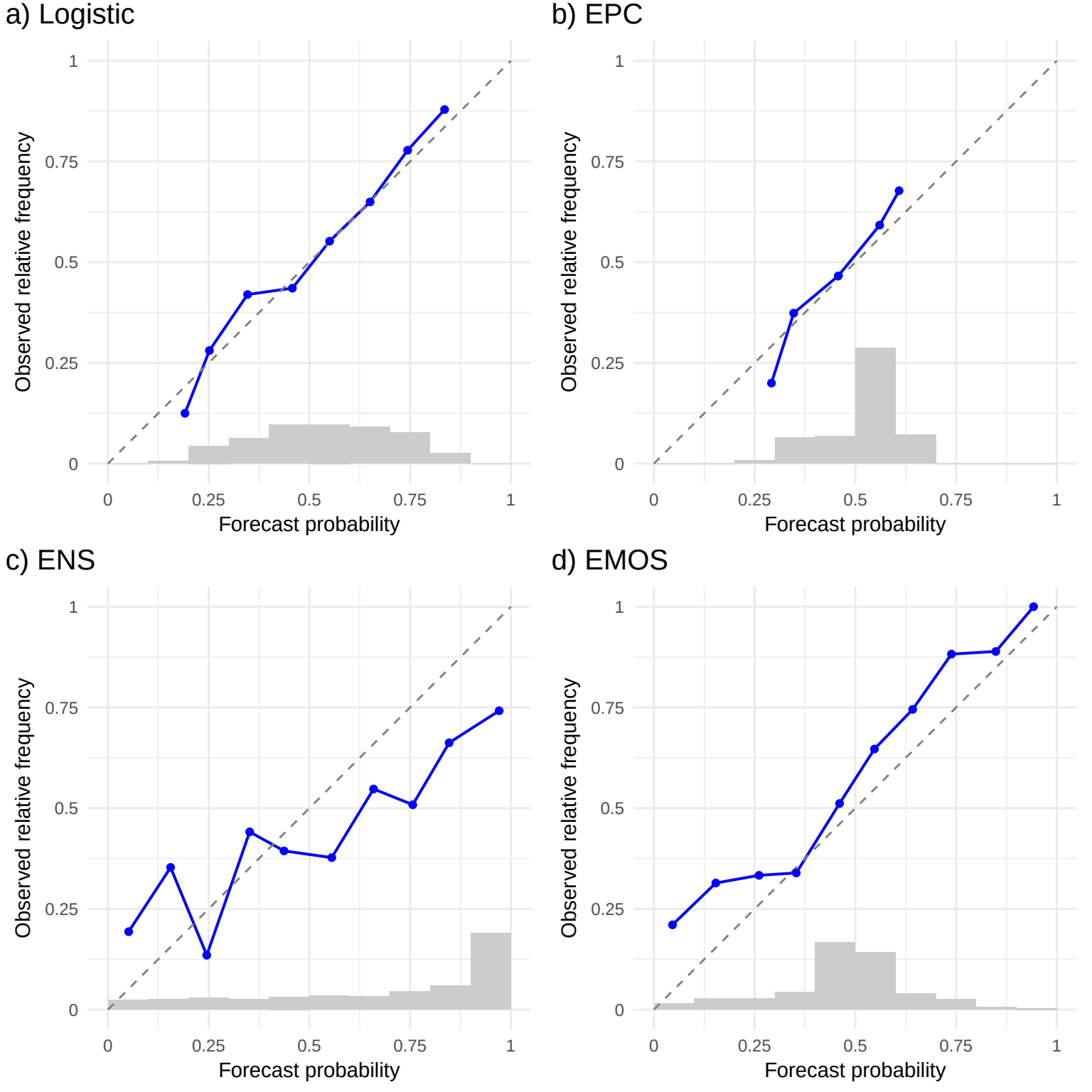
a) Logistic
b) EPC
c) ENS
d) EMOS
Observed relative frequency
Forecast probability
0
0.25
0.5
0.75
1

Figure 4.

a) Logistic vs. EPC

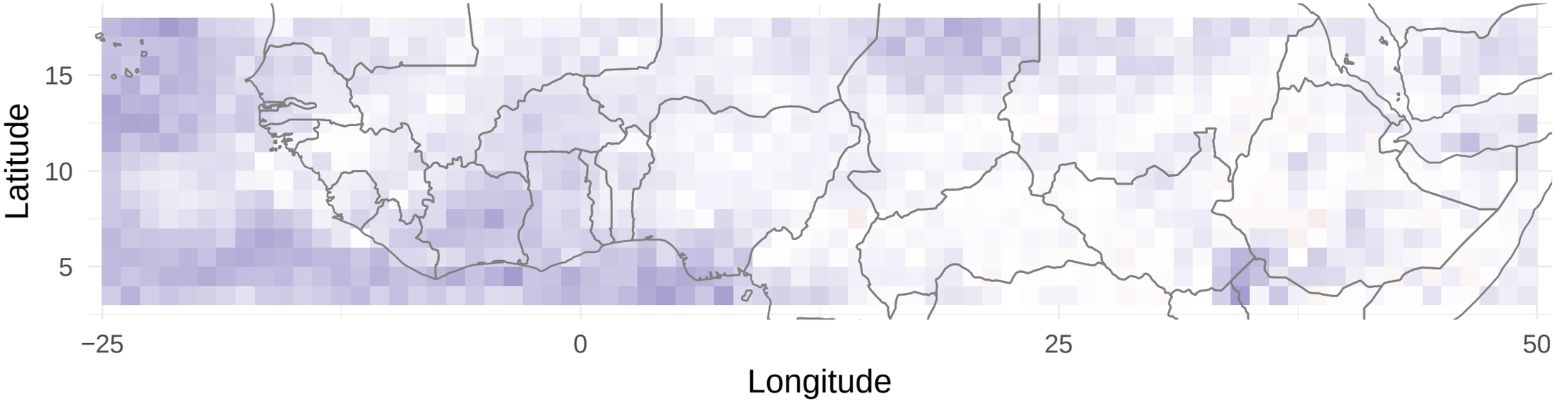

b) Logistic vs. EMOS